

This paper was presented at the 24th International Workshop on Human Subjects for Biomechanical Research. The contents have not been screened for accuracy by a peer review process; thus this paper should not be referenced in the scientific literature.

***In Situ* Measurement of Loads in the Tibia**

Kelly B. Kennett
Failure Analysis Associates

Jeff R. Crandall, Cameron R. Bass, Gregory S. Klopp
Department of Mechanical, Aerospace, and Nuclear Engineering
University of Virginia

Abstract

This paper documents the development and initial benchmarking of a technique for measuring *in situ* loads in the human tibia during impact testing. The technique entails removing a section of the tibia from the leg and replacing it with an implantable tibial load cell derived from those found in anthropomorphic test dummies. Mounting of the load cell inside the leg is accomplished by mating the instrument through a reusable cradle to disposable metallic cups. The cups are positioned around the cut ends of the tibia and cast in place with epoxy. Quasi-static tests, loading tibias and full legs in axial compression and anterior-posterior bending, were conducted in order to verify that the technique is capable of measuring the desired loads without compromising or drastically altering the function of the leg.

Introduction

Lower extremity injuries have recently come to the foreground in automotive safety research as one of the most common and debilitating, though not typically life threatening, injuries found in crash occupants. The desire to mitigate these injuries has spawned research into the injury tolerance and behavior of the lower leg, ankle, and foot. A prerequisite for developing more biofidelic dummies as well as new injury criteria is being able to accurately and reliably measure the forces that are present in the leg during both injurious and non-injurious cadaver testing. This paper documents the development and benchmarking of an instrumentation technique for measuring *in situ* loads in cadaver tibias.

In situ tibial load cells are common in Hybrid III test dummies. Working at the behest of the University of Virginia, Robert A. Denton, Inc. manufactured a similar tibial load cell for implantation into the human tibia. These instruments measure three forces and two moments passing through the load cell. They were not designed to measure torsional moment about the load cell's long axis because the initial intermedullary rod mounting scheme, described in the next section, did not resist that degree of freedom. Figure 1 shows the exterior dimensions of the load cell.

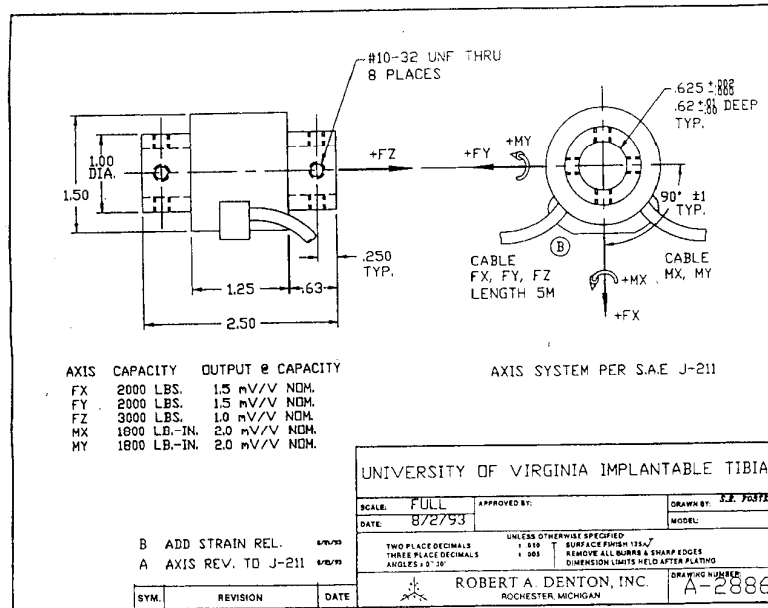


Figure 1 Tibial Load Cell Exterior Dimensions

By definition, an *in situ* load cell requires the removal of a section of tibia, and implantation of the load cell in its place. The mounting flanges of the load cell were originally designed to accommodate 1.59 cm (5/8 in.) rods, which would be threaded into the medullary canals of the tibia at the site of insertion. This mounting technique, referred to as the intermedullary (IM) rod scheme, entailed removing a section of tibia slightly larger than the length of the load cell, drilling and tapping the medullary canals near the removed section, inserting the rods, and then securing the load cell to the rods with set screws. The fibula was left intact.

A total of eight full cadavers had tibial load cells implanted with this method. During the sled tests of these cadavers, 8/16 of the legs sustained one or more artifactual fractures due to the presence of the load cells. The typical artifactual fracture pattern, shown in figure 2, indicated a failure brought about principally by anterior-posterior bending loads. Basically, bending loads applied to the tibia would pry the IM rod out of the bone. Furthermore, the data from the load cells indicated that these injuries were occurring at loads substantially below those recorded in similar dummy testing. During the course of testing these eight cadavers, a number of measures were tried in an attempt to shore up this mounting technique. These measures included introducing epoxy into the medullary canals with the rods, adding circumferential clamps to the cut tibia ends, and facing the tibial load cell flange directly up to the cut bone faces through the use of spacers. None of these measures mitigated the problem.

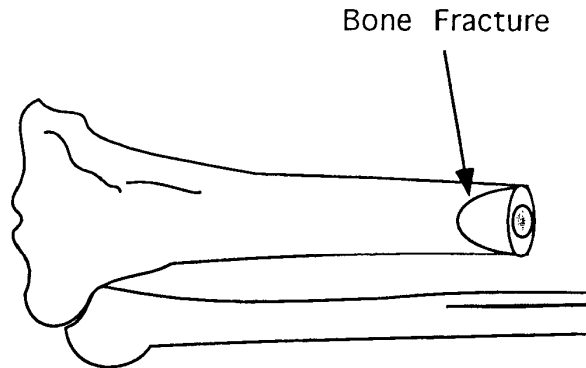


Figure 2 Typical Artifactual Injury Pattern with IM Rod Mounts

Modeling on Bone-Load Cell Interface

The artifactual injuries created by the initial IM rod tibial load cell mounts necessitated a better understanding of the load cell-bone interface in order to design an improved load cell mount. Consequently, a finite element model of the tibial shaft with various end loading conditions was created to investigate load transmission and concentration patterns in the region of the cut bone face.

The geometry of the tibia cross-section used in the model was determined by Piziali, Hight, and Nagel (1980) and suggested by them as suitable for a finite element model. The tibial cross-section used in the model was taken from the mid-diaphysis cross-section data given in their paper. Since the region of interest for the load cell mounts was entirely within the diaphysis of the tibia, the cross-section of the bone was assumed to be constant. The data of Piziali, et al. indicated that this was a reasonable assumption in the center 60% of the tibial diaphysis.

Bone is a nonhomogeneous, viscoelastic material with anisotropic properties. Cortical bone, however, can be effectively modeled as a transversely isotropic material (Cowin, et al. 1987). The material constants for cortical bone found in Cowin were utilized in the model. The center of the tibia cross-section ordinarily contains cancellous bone. The mechanical properties of cancellous bone are an order of magnitude less than those of cortical bone (ibid.); thus, for simplicity, the cancellous bone was ignored and the center of the tibia cross-section left hollow in the model.

The load cases chosen for application to the different load cell mount models were derived from the tibia loads previously found in dummy and cadaver leg pendulum and sled tests at the UVA. The principal load of interest, the apparent failure load for the intermedullary rod mounts, was anterior-posterior (A-P) bending. A-P shear loads and axial compressive loads were later included in the model to represent the most general case of impact loads found in the automotive crash environment. The results for each model are displayed graphically in terms of the Von Mises equivalent stress, or the square root of the distortion energy density, in order to reveal areas of load concentrations and well-behaved load transmission.

The model of the IM rod mounting technique was created using a steel rod of 1.59 cm (5/8 in.) in diameter inserted into the hollow medullary canal portion of the tibia shaft model.

The rod was inserted into the canal to a depth of 1.90 cm from the bone face. The rod and bone were given perfect connections at the matching nodes, representing the best case scenario for the mating of the actual rod and bone threads, thus allowing the threaded rod mounting scheme to be evaluated in its optimal condition. The remote end of the bone shaft model was fixed. Figure 3 represents the output for the IM rods with only an A-P bending load of 70 N*m applied. The threaded rod mounts created an abrupt transfer of load at the termination of the rod in the bone on the inside diameter of the bone. The cut bone face must bear no load at its boundary, as the model depicts. However, the bone's cortical shell does not develop substantial load until the rod terminates, whereby a stress concentration develops in the bone model on the interior of its cross-section. Virtually no load is borne by the first 0.75 cm of the bone longitudinally from the cut face. The maximum Von Mises stress, with a magnitude of 55 MN/m², develops on the posterior face of the tibia coincident with the termination of the mounting rod. When the shear and axial loads were added to the model, the stress concentration at the termination of the rod was exacerbated, particularly in response to the introduction of the shear load. The stress concentrations and load patterns observed in the model output agreed well with the observed failure modes for those tibias with artifactual injuries due to the IM rod mounts. Furthermore, this model was also used to determine that a clamping force applied around the bone's circumference near the cut face was not capable of effectively attenuating the irregular load transmission and subsequent stress concentrations found with the IM rod mounts.

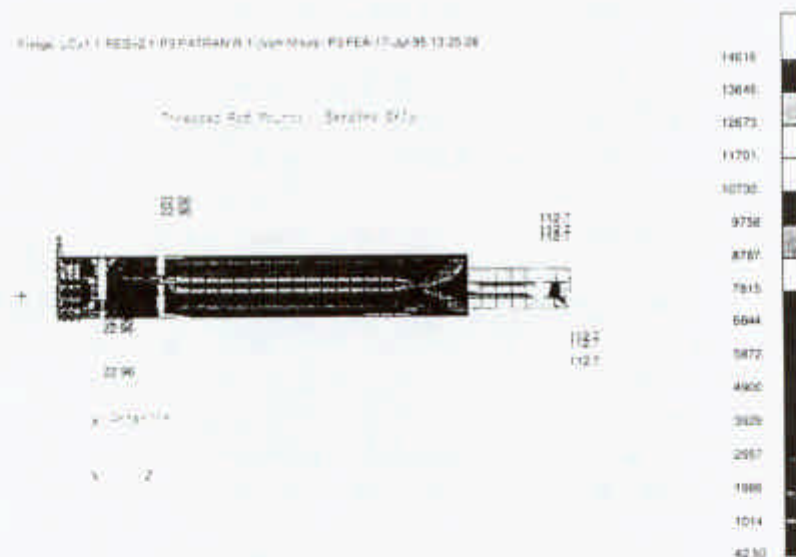


Figure 3 Model Output: IM Rod Mount - Bending Only

The FE model was used to evaluate a number of alternative mounting schemes. Ultimately, an exterior cup surrounding the cut bone end and filled with a hardenable epoxy material was chosen for the load cell mount. This exterior mounting scheme makes use of the bone's hard cortical shell and allows load transmission to the cut bone end through the solid end cap on the cup. For the FE evaluation of this new mounting concept, the exterior cup was modeled as a 5.080 cm diameter steel cup with 0.127 cm wall thickness. The cup extended 3.175

cm over the cut bone end. In contrast to the previous IM rod model where the remote end of the bone was fixed, the end face of the cup was fixed rigidly as a boundary condition, simulating the attachment of the cup mount to the load cell. The material properties chosen for the filler substance in the model were those of molded nylon, taken as a representative polymer. The medullary canal was left empty in the model. Equivalent load cases as those applied to the IM rod model were also applied to the exterior cup mount model.

Figure 4 shows the Von Mises stress results for the bending only load case applied to the exterior cup mount model. Under this loading, the maximum Von Mises stress develops in the tibia model approximately 0.3 cm past the end of the mount on the outer, anterior surface of the bone. In this case, the distortion energy density, or Von Mises stress, was only 27.6 MN/m². This represents a 50% reduction in the maximum Von Mises stress from the IM rod mounting case with bending only. Moreover, the transition of load from the mount to the bone generates no abrupt load changes. The bone begins to bear load at the contact between the cut face and the cup. The general load case of bending, shear, and axial forces was also applied to this model. With all three loads applied, the maximum Von Mises stress was reduced by 10% from that found for the same loading with the IM rod. Although this reduction is not as substantial as the bending only case, the load transmission pattern with the exterior cup includes no abrupt stress changes, while the maximum stress develops on the harder exterior cortical shell of the bone.

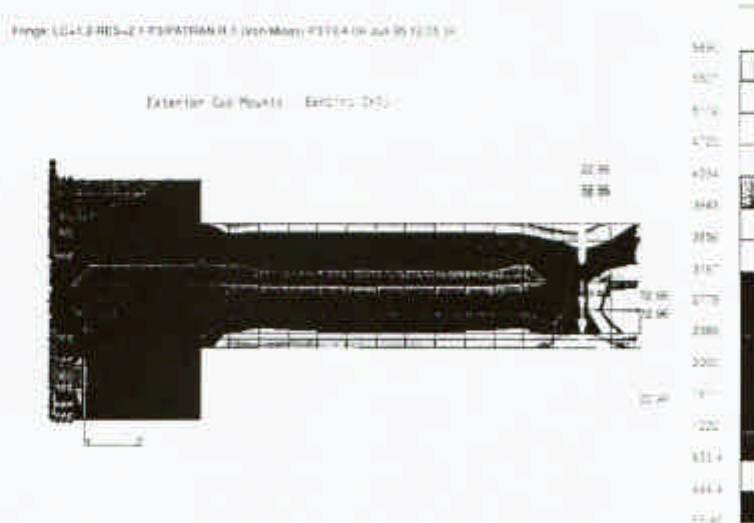


Figure 4 Model Output: Exterior Cup Mount - Bending Only

Exterior Cup Load Cell Mount Design

The FE results indicated that an exterior cup fixed to the cut bone ends would adequately transmit the loads to and from the tibial load cells, avoiding the stress concentrations that created the artifactual injuries seen previously. Thus, an exterior cup mount for the load cells was designed. The need to fill the metal cups with an epoxy material to mate them to the bone ends led to two important design features of the final mounts. First, the insides of the metal cups would need to be scored so that the epoxy would mechanically 'bond' to the cups, providing

torsional stability of the epoxy plugs within the cups. Second, the cups would not be easily removable from the bone ends after testing, thus they must be disposable, while still mating with the existing tibial load cells. This requirement for disposable cups led to a final two-part mount design including a simple metal cup epoxied to the bone, which fastens to a reusable load cell 'cradle' which attaches the load cell to the fixed cup. This final design is shown schematically in figure 5.

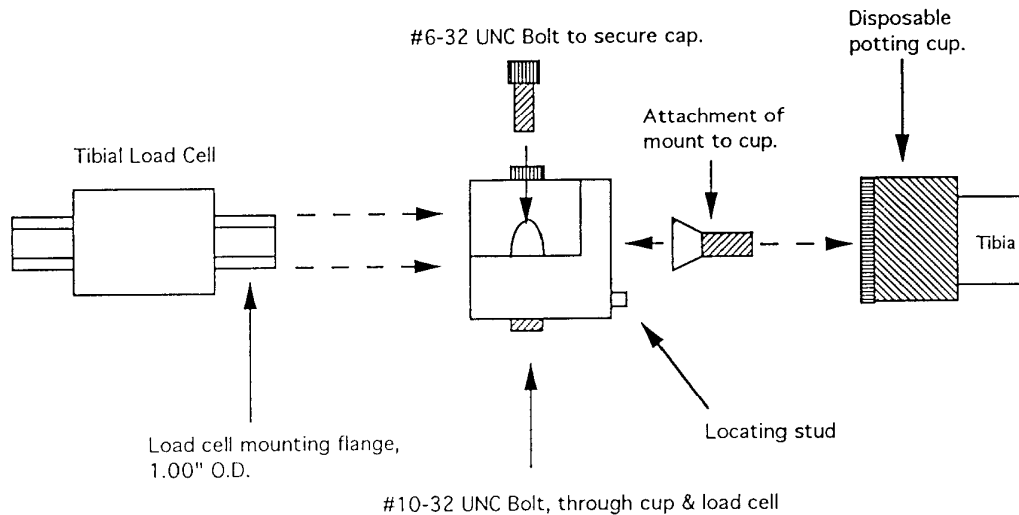


Figure 5 Exterior Bone Cup/Load Cell Cradle Mounting Schematic

The load cell's mounting flange mates flush with the solid end of the 'cradle', while the solid end of the 'cradle' and the cup mount flush together. Finally, the cut bone end rests flat against the inside surface of the disposable cup's end cap. Thus there is a direct load transmission path between the cut bone ends and the load cell housing. The final inside diameter chosen for the disposable cups is varied to fit the individual specimen, while the depth of the cups is approximately equal to 3.2 cm. The reusable cradle, whose inside diameter matches the 2.54 cm outside diameter of the tibial load cells, incorporates a removable 'cap' so that the load cell can be inserted directly at the time of testing. For multiple isolated limb tests on a pendulum system, this setup allows the sequential testing of many specimens with a limited number of actual load cells. Furthermore, blank aluminum cylinders with the same length and flange diameter as the load cells can be used during the mounting process, thus reducing the chemical exposure to the load cells.

The final design requires that 8.9 cm of the tibial diaphysis be removed. A detailed surgical procedure for the insertion of the load cell mounts can be found in Kennett (1995). Once the bone section is removed, the surface of the bone ends must be desiccated for the epoxy filler to bond to the bone. The disposable cups, mounted on the reusable cradles, are then filled with slow-cure, low shrinkage, low heat epoxy, thickened with an inert agent such as glass beads or sand to retain the epoxy in the cups during the curing process. Once the cups, with the accompanying cradles, are mounted on the bone ends, the aluminum blanks are inserted in place

of the load cells to facilitate aligning the tibia in its anatomic position. Splinting of the limb is required during the curing process to maintain this anatomic position. Once the epoxy has hardened, the blanks can be removed. When the load cells are inserted, the tibia will be returned to the same position.

A notable feature of this measurement and mounting technique is that the fibula is left intact and not disturbed from its normal anatomic position. Leaving the fibula intact is important for maintaining the overall alignment in the leg, natural load distribution between the bones, and ankle mortise geometry in the joint. Discussions of the function of the fibula can be found in Lambert (1971), Takebe, et al. (1984), Skraba and Greenwald (1984), and Weinert, et al. (1973).

Axial Testing

The presence of the tibial load cell in the lower leg of a cadaver alters significantly the structure of the limb, and could alter the biofidelic response of the limb when tested in impact conditions. A series of quasi-static axial and bending tests were performed in order to evaluate first whether the exterior cup mounting method was capable of bearing loads of the magnitudes found in crash tests without creating artifactual injuries as the IM rod mounts did. Second, the tests were to evaluate whether this altered structure would exhibit similar mechanical characteristics to tests on undisturbed cadaveric specimens, both in this study and in those reported in the literature.

All axial loading tests were performed quasi-statically on a Tinius-Olsen Universal Test machine. Load and displacement data were taken from the test machine, while data from all five tibial load cell channels were acquired where applicable. Table 1 presents a summary of the axial loading tests performed.

Specimen Type	Limbs Tested	Tests Performed
Extracted, denuded tibia	Single bone	Ramp up to designated load and hold; constant displacement rate to failure
Above-knee, cadaver limb amputations	One right leg, one left leg, each with and without load cell	Ramp up to designated loads and hold for 10 sec., 4 loads
At-knee, cadaver limb amputations	Two pairs of limbs, left legs with load cells, right legs without	Ramp up to designated loads and hold for 10 sec., 4 loads; constant displacement rate to failure

Table 1 Axial Test Summary

The first test performed on a tibia mounted with the exterior cup scheme was a simple axial load applied at a constant displacement rate on an extracted, denuded bone. The proximal and distal ends of the bones were cast into epoxy caps for loading surfaces. When the bone was compressed axially to 5100 N, failure began at the distal end inside the epoxy cap. In this test,

the bone exhibited an overall stiffness prior to initial failure of 1240 N/mm. The loading on this bone was continued beyond initial failure to an ultimate maximum load of 7200 N, during which the bone yielded at both proximal and distal ends inside the epoxy caps, but did not fail, shift, or deform at the mounting site of the load cell. The results of this test led to the conclusion that the exterior cup mounting scheme was ready for further, *in situ*, testing in amputated limbs.

Three sets of quasi-static axial load tests were performed on cadaveric limbs to both evaluate the 'loading error' due to the tibial load cells and gather data for comparison on lower limb mechanical properties. For the first set of tests, two legs, amputated in the distal third of the femur, were loaded without the load cell present, then again with the load cell in place. The legs were loaded vertically through the knee, with the knee held in approximately 90 degrees of flexion. The distal third of the thigh was held in place by a concave fixture attached to the loading crosshead of the test machine. Inversion and eversion motions of the ankles were restricted by placing plates on both the medial and lateral sides of the foot ankle complex. These plates did not restrict the dorsiflexion/plantarflexion motion or the axial compliance of the ankle. The legs were loaded in a ramp and hold pattern, a representative plot of which is shown in figure 6. This pattern was used so that manual ankle displacement measurements could be made at regular intervals. Markers for measuring the ankle displacements were imbedded into the medial malleolus of each of the two specimens. The second and third sets of tests were conducted using two contralateral pairs of limbs amputated at the knee. The tibial plateaus of the limbs were cast into epoxy caps to create a regular loading surface. The right leg of each pair was left otherwise intact, while the left legs were mounted with the tibial load cells. The second set of tests consisted of loading these limbs in the same ramp and hold pattern as that just described. The third set of tests consisted on one uninterrupted load to failure, during which no ankle measurements were made. Table 2 presents a summary of the data from these three sets of tests.

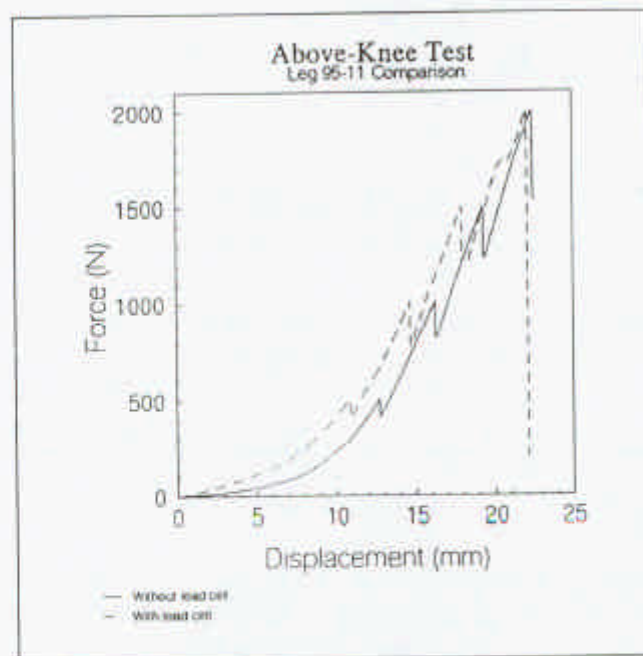


Figure 6 Representative 'Ramp and Hold' Loading Pattern

Leg	Stiffness at Ankle (N/mm)	Overall Stiffness (N/mm)	Max. Shear Resultant (N)	Max. A/P Bending (N*m)	Failure Load (N)
Ramp and Hold Tests - Above Knee Amputations					
95-11 w/o lc	270	160	----	----	----
95-11 w/ lc	220	140	104	31	----
95-12 w/o lc	145	85	----	----	----
95-12 w/ lc	160	80	199	29	----
Ramp and Hold Tests - At Knee Amputations					
Lefts = with load cell, Rights = without load cell					
95-13 L	710	560	193	1.3	----
95-13 R	800	480	----	----	----
741 L	360	370	182	2.2	----
741 R	400	390	----	----	----
Failure Tests - At Knee Amputations					
Lefts = with load cell, Rights = without load cell					
95-13 L	----	1053	775	67	8500
95-13 R	----	1020	----	----	8680
741 L	----	565	360	72	4550
741 R	----	612	----	----	4210

Table 2 Axial Test Data Summary

Although the ankle stiffnesses are not directly dependent on the presence or absence of the tibial load cells, they can be viewed as indicators of the overall variability within the tests and among the specimens. Physically, the stiffness measured at the ankle must be higher than the measured overall stiffness. This is true for each case with the exception of 741L. Ankle stiffness errors were estimated to be ± 20 N/mm, 95% confidence interval. Given the error band for the measurements, this case does not present a physical paradox. Draeger (1945) conducted one similar test on cadaver limb and measured 610 N/mm stiffness at the ankle. Hirsch and White (1965) conducted these type tests on five human volunteers, keeping the loads below three times body weight per leg. For their volunteers, aged 19 to 26 years, they found an average ankle stiffness of 403 N/mm, with a range of 300-700 N/mm. The range for the tests reported here, 145-800 N/mm, encompasses that of Hirsch and White. Although specific age data were not available on the cadaveric specimens in this study, observation indicates that none falls within the age range tested by Hirsch and White. Bone and soft tissue differences due to the specimen age, as well as postmortem changes and passive musculature effects in *in vivo* tests, certainly may play a role in the differences between these findings and those of Hirsch and White.

Any lower extremity stiffness differences due to the tibial load cells were obscured by the compliance of the knee and accompanying soft tissues in the above-knee amputation cases. Although the values for the overall stiffness of both limbs in these tests were much lower than

the ankle stiffnesses, there were no statistically significant changes in the values subsequent to the introduction of the load cells. For the at-knee tests, if the tibia-fibula complex is much stiffer than the plantar arch of the foot and the ankle joint, the overall and ankle stiffness values should agree. In the case of 741 L & R, this is true. Furthermore, there were not detectable differences due to the load cell in the left leg. For 95-13 L & R, the compliance of the tibia/fibula pair was not negligible in relation to the foot/ankle complex. Also, the right leg, without the load cell, was less stiff than the left with the load cell. This is likely due the fact that the section of tibia removed for the load cell was more compliant than the metallic load cell and mounting structure. For axial loading through a well-aligned mount, the cut faces of the tibia should directly load the metal structure and not the epoxy filler in the cups. For all of the axial tests, the off-axis shear forces and bending moments measured by the tibial load cell were small. This indicates a good alignment and fixation of the legs mounted with the load cells.

Bending Tests

Anterior-posterior bending of the tibia, after axial force, is the second load of central interest in the dynamic crash environment. In order to evaluate the tibial load cell's effect on the bending strength, stiffness, and strain patterns of the tibia, one single tibia and two contralateral pairs of denuded, extracted tibias were tested quasi-statically in three-point bending. All tests in this study were conducted in the A/P direction; however Yamada (1970) states that there is no discernible difference in the ultimate tibia bending load in the medial/lateral (M/L) direction. Minns, et al. (1975) found an approximately constant ratio of 1.6 for A/P to M/L bending stiffness for the tibia.

In preparation for testing, epoxy rings approximately 1 cm thick and 10 cm in diameter were cast around both the distal and proximal ends of each bone. The rings were cast with the bone in a jig which ensured that the plane of the rings was perpendicular to the long axis of the bone and that the centers of the two rings coincided. In order to reduce stress concentrations directly under the application of the load, the load applicator, attached to the universal test machine, was a metal cylinder of 1.27 cm diameter.

The single, unpaired bone was tested first in bending with the tibial load cell in place to both verify the test method and the capability of the exterior cup mounts to withstand substantial bending loads. This bone was tested once to failure, yielding at 108 N*m in the center of the bone's span under 2209 N applied by the loading crosshead. The tibia failed at its distal cut face, inside the cup filled with epoxy. The epoxy filler did not yield.

For the two contralateral pairs of bones, each left tibia was tested non-destructively twice, once without and once with the load cell. The left tibias were both mounted with strain gages in order to evaluate, with the introduction of the load cell, the changes in strain pattern found in the bone away from the tibial load cell mounting sites. Four gages were installed on each bone, one each on the distal and proximal ends on both the anterior-medial face and the posterior face of the bone. The gages were aligned to measure strain axially along the long axis of bone and positioned as far as practical from the region of the load cell mounts. The non-destructive load cycle was repeated 10 times for each bone. Pair 93-35 comes from a 57 year old, 61.7 kg female who died of complications related to hypertension. Pair 92-13 comes from a 62 year old, 70.8 kg male who died of cardio-pulmonary arrest brought on by heart disease. Table 4 below summarizes the average data for these 10 cycles for each left tibia, both with and without the load cell.

Test	A/P Moment (N*m)	Strain ($\times 10^{-6}$)			
		Ant.-Med. Distal	Posterior Distal	Ant.-Med. Proximal	Posterior Proximal
93-35 L w/o lc	25	-196	299	-134	99
93-35 L w/ lc	21	-188	379	-129	178
92-13 L w/o lc	43	-276	401	-104	212
92-13 L w/ lc	40	-248	375	-79	185

Table 4 Non-destructive A/P Bending Strain Summary

Within each individual set of 10 cycles, the strain data was quite repeatable and no permanent deformations were noted, indicating elastic response from the bones. For 93-35 L, although the anterior strains remain relatively unchanged, the posterior strains were increased substantially, by 26% distally and 80% proximally. For 92-13 L, the strains were either essentially constant, or reduced slightly. These results suggest that, at least for 93-35 L, the cut bone ends inside the epoxy filled cups were capable of some non-planar deflections, referred to as warping.

Subsequent to these tests, both pairs of bones were tested once to failure: the lefts with the load cells; the rights without. Table 5 presents these results.

Test	Max. Moment (N*m)	Max. Shear (N)	Displace- ment (mm)	Stiffness (N*m/mm)	Posterior Distal ϵ ($\times 10^{-6}$)	Ant.-Med Prox. ϵ ($\times 10^{-6}$)
93-35L w/ lc	184	1549	11.1	16.6	2152	186
93-35R w/o lc	74	647	8.1	9.1	----	----
92-13L w/ lc	234	1702	22.2	10.5	2180	519
92-13R w/o lc	438	3188	11.6	37.8	----	----

Table 5 Bending Failure Test Summary

For the bones of subject 93-35, the smaller tibias of the two pairs, the presence of the load cell greatly increased the breaking strength of the tibia. With the weakest portion of the bone removed, the load was forced to build up to the failure load of the stronger portions of the bone contained in the mounting cups. In general, as the age of adults increases, the breaking strength of their bones decreases, especially in females. This trend may explain the low breaking load of 93-35 R, the intact specimen.

For the bones of subject 92-13, the presence of the tibial load cells nearly halved the breaking strength of the tibia. However, the bones of 92-13 were remarkably large bones. The typical breaking strength of adult human tibias in three-point bending is 2160-2940 N applied load (Yamada, 1970), which translates into 154-209 N*m for subject 92-13's anthropometry. The 438 N*m breaking load for 92-13 R, without tibial load cell, is more than twice as large as

the upper end of the published range. Yamada also reports an average ultimate deflection for adult human tibias in three-point bending of 9.0 mm. For all bones except 92-13 L, the displacements at failure agree well with this number. 92-13 L deflected a great deal while the proximal section was failing by rotating and pulling out of the mounting cup. The failure criterion for stopping the test was a drop in applied load, which did not take place until after the tibia had begun to deform permanently by the proximal section wedging itself into the mounting cup. The displacement of the loading crosshead at the beginning of the permanent deformation was not recorded; however, it was substantially less than the 22.2 mm shown in table 5. The conclusion of the bending failure tests is thus that the tibial load cells increase the ultimate bending load of small tibias, while they decrease the ultimate bending load of large tibias. All of the bending loads to failure reported for these tests are above the typical loads found in the dynamic sled tests at UVA. For this reason, the changes in the bending response of the tibia as a result of the implantation of the load cell are not expected to adversely affect dynamic sled test results.

Conclusions

The work documented in this paper entails some of the foundation necessary for the full scale use of the *in situ* tibial load cell in human cadaver impact testing. With the assistance of a finite element model, a mechanically sound method of mounting the load cells in human tibias was developed. Through quasi-static axial and bending tests, the exterior cup mounting method has been shown to be capable of withstanding the loads typically found in full scale impact tests without generating artifactual injuries in the tibia. However, these same tests also indicate that the presence of the load cell in the bone can alter the injury pattern of the tibia itself. Consequently, this measurement technique can be effectively used to investigate injury tolerances for the foot and ankle, as well as the knee and femur, but should not be used to research tolerances of the lower leg itself.

Subsequent to the research presented in this paper, more than 30 cadaver lower limbs have been mounted and loaded dynamically in sled and pendulum tests using this method at the University of Virginia. None of these limbs has experienced an artifactual injury due to the tibial cells or their mounts. This technique has also been recently applied to the humerus in order to measure the loads in the upper arm during airbag deployment.

References

- Cowin, S., VanBuskirk, W., Ashman, R., "Properties of Bone," in *Handbook of Bioengineering*, R. Skalak and S. Chien, editors, McGraw Hill: New York, 1987.
- Draeger, R. H., et. al., "A Study of Personnel Injury by Solid Blast and the Design and Evaluation of Protective Devices," Report No. 1, Research Project X-517, Naval Medical Research Institute, March, 1945.
- Hirsch, A. E., White, L. A., "Mechanical Stiffness of Man's Lower Limbs," ASME Winter Congress, Transactions of the American Society of Mechanical Engineers, 1965.
- Kennett, K. B., *The Development and Evaluation of an In Situ Tibial Load Cell*, University of Virginia Master's Thesis, August, 1995.
- Lambert, K. L., "The Weight-Bearing Function of the Fibula," *The Journal of Bone and Joint Surgery*, vol. 53-A, no. 3, 1971.

-
- Minns, R. J., Campbell, J., Bremble, G. R., "The Bending Stiffness of the Human Tibia," *Calcified Tissue Research*, vol. 17, pp. 165-168, 1975.
- Piziali, R. L., Hight, T. K., Nagel, D. A., "Geometric Properties of Human Leg Bones," *Journal of Biomechanics*, vol. 13, pp. 881-885, 1980.
- Skraba, J.S., Greenwald, A. S., "The Role of the Interosseous Membrane on Tibiofibular Weightbearing," *Foot and Ankle*, vol. 4, no. 6, pp 301-304, 1984.
- Takebe, K., Nakagawa, A., Minami, H., Kanazawa, H., Hirohata, K., "Role of the Fibula in Weight Bearing," *Clinical Orthopaedics and Related Research*, vol. 184, pp. 289-292, 1984.
- Weinert, C. R. Jr., McMaster, J. H., Ferguson, R. J., "Dynamic Function of the Human Fibula," *The American Journal of Anatomy*, vol. 138, pp. 145-150, 1973.
- Yamada, H., edited by Evans, F. G., *Strength of Biological Materials*, Williams and Wilkins Co.: Baltimore, 1970.

DISCUSSION

PAPER: **In Situ Measurement of Loads in the Tibia**

PRESENTER: Kelly Kennett, Failure Analysis Associates, Inc.

QUESTION: Guy Nusholtz, Chrysler Corporation

You may have mentioned it but how much difference was there between the tibia with the tibia load cell and the tibia without it in terms of its response? You mentioned that there was some difference and that you think that it's a good representation but how much of an error would we expect to see?

A: In loads where the principal loading is axial, I would say that you can suspect virtually undetectable differences. The differences between human ankles and knees and the stiffness associated with that is going to dominate the response of the leg. In the bending response, the displacement to failure tends to be relatively well represented with what is in the literature. On the other hand, the load that corresponds to that displacement, is changed substantially and as I showed you, it varies between bone quality and bone size as well. In very large bones, their ultimate strength can be reduced. In smaller bones, their ultimate strength is actually increased because you've excised that minimum moment of inertia.

Q: Did you do any checks in the load cell where you put the load cell and then you had another load cell under the foot, compress the system?

A: Well, that's essentially how we extracted the tibial weight bearing percentage, in that, in our at knee axial tests, when you load up with the test fixture, you have the overall applied load. Certainly, it's a determinate structure if you know all the loads in the tibia, you can pretty much at least hypothesize what axial load's going to the fibula. So, in that way, we've, I guess verified that we're getting the right axial loads by saying the loads that if you account for a normal percentage found in the fibula, as quoted in the literature, then the sum of all that adds up to what we found in the literature.

Q: Assuming that you've got a representative axial load, you have some sort of error in your bending moments, in the comparisons with the Hybrid III and the ALEX, did you try and dissect that out to see whether you were getting contamination from the bending moments.

A: No. As I understand your question, I don't think that work has been done yet. No.

Q: OK. Thank you.

